

Electronic Supplementary Information

Maximum hydrogen chemisorption on KL zeolite supported Pt clusters

Christopher Jensen,^a Doris Buck,^a Herbert Dilger,^a Matthias Bauer,^b Fritz Phillipp^c and Emil Roduner^{*a}

^a Institute of Physical Chemistry, University of Stuttgart, Pfaffenwaldring 55, 70569 Stuttgart, Germany. Fax: 49 711 68564495; Tel: 49 711 68564490; E-mail: e.roduner@ipc.uni-stuttgart.de

^b Faculty of Chemistry, Technical University of Kaiserslautern, Erwin-Schrödinger-Str. 54, 67663 Kaiserslautern, Germany.

^c Max Planck Institute for Intelligent Systems, Heisenbergstr. 3, 70569 Stuttgart, Germany.

Details of sample preparation:

KL zeolite was obtained from Chemie Uetikon AG (CU) in Switzerland, and in view of magnetization measurements an iron-free KL zeolite was obtained from Süd Chemie AG (SC) in Germany. The zeolites were calcined in air to burn off any residual organic impurities. To exchange any ions other than K^+ 5 g KL zeolite were stirred in 125 ml of 1 M aqueous KCl solution at room temperature (RT) for 24 h. The zeolite was filtered off, washed with doubly distilled water to remove Cl^- ions, and dried in an oven at 353 K overnight. This step was repeated three times. Chemical analysis using ICP-OES resulted in Si/Al = 3.0 and K/Al = 0.98 for KL(CU) zeolite, and Si/Al = 2.8 and K/Al = 0.98 KL(SC) zeolite. Pt/KL zeolites were prepared by aqueous ion exchange with 3 mM solution of $[Pt(NH_3)_4]Cl_2$ (Aldrich) that was added dropwise to a flask containing a suspension of 1 g KL zeolite in 500 ml of water which was stirred for at least 3 days at 343 K. The exchanged zeolite was filtered, washed again with doubly distilled water, and dried overnight in an oven at 353 K. This procedure led to a Pt content of 5.3 wt% (CU) and 5.5 wt% (SC), and for both zeolites to a K/Al ratio of ~ 0.72 , showing the extent of exchange with Pt. Calcination was carried out in flowing O_2 (120 ml min^{-1}) using a heating rate of 0.5 K min^{-1} from RT to 623 K and holding this temperature for 5 h. After the sample had cooled to RT, residual O_2 in the reactor was purged with N_2 . Reduction was then performed in flowing H_2 (80 ml min^{-1}) at a heating rate of 4 K min^{-1} from RT to 503 K and keeping the sample at 503 K for 1 h. After the sample had cooled to RT in hydrogen atmosphere, the reactor was purged with N_2 , and the samples were transferred to EPR tubes in a glove box under nitrogen atmosphere, and then evacuated.

X-Band EPR spectra were recorded on a Bruker EMX spectrometer with a microwave frequency and power of about 9.47 GHz and 1.01 mW at 4 K. The spin concentration of a Pt/KL sample was calibrated against a standard sample (ultramarine blue diluted by KCl).

Characterization by EPR:

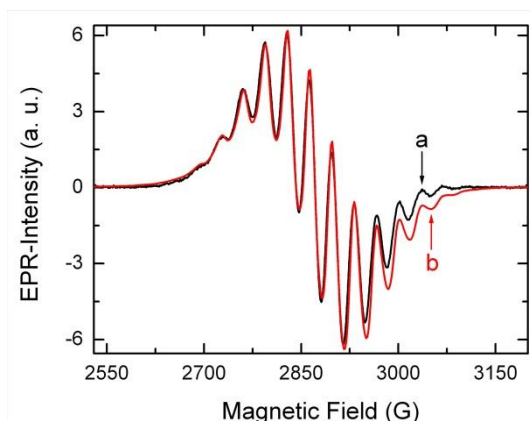


Figure S1 a) EPR spectrum of a partially hydrogen covered Pt_{13} cluster supported on KL(CU) zeolite. b) Simulation using the parameters $g_{\perp} = 2.3528$, $g_{\parallel} = 2.3729$, Pt hyperfine splitting due to 12 equivalent nuclei with $A_{\perp} = 67.1 \text{ G}$, $A_{\parallel} = 68.1 \text{ G}$ and an intrinsic (single-crystal) line width of 9 G.

The multiplet represents a platinum species since its g value is much larger than g_e of the free electron, as expected for unpaired electrons in a more than half-filled d-shell of simple transition metal centers.¹ Isotopically enriched Pt samples proved unambiguously that the splitting is due to Pt.²

Characterization by HRTEM:

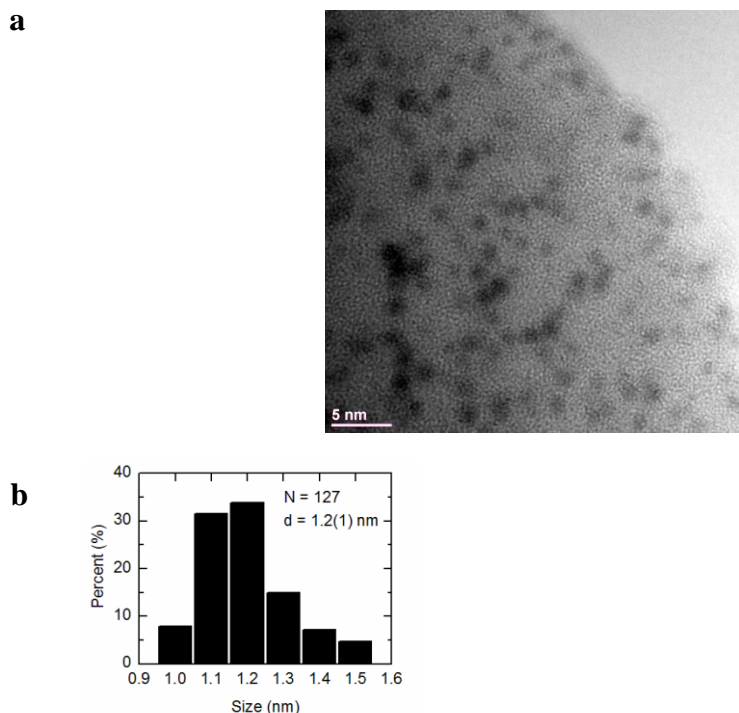


Figure S2 (a) HRTEM image of a 5.3 wt% Pt/KL(CU) sample showing the dispersion of the Pt particles (black dots) in the zeolite after initial hydrogen reduction. **(b)** Histogram of size distribution.

The particle sizes were measured from intensity profiles of a set of five images across their contrasts using Digital MicrographTM software. Only the contrasts of well isolated particles in thin specimen areas were measured in order to avoid artefacts due to clustering or projection effects. The mean value indicated in Figure 3b overestimates the true mean particle size, since the contrast of particles of 1 nm and smaller is too weak to be measured reliably. This manifests itself also in an asymmetry of the histogram. The weak contrast and blurred images result partly from the embedding of the small particles within the zeolite.

Details of the EXAFS experiment and data treatment:

EXAFS samples were stored in a glove-box with an atmosphere of H₂O <0.1 ppm and O₂ <0.1 ppm, and filled in a container gas tight up to 200 bar. No further treatment with H₂ prior to the measurements was carried out in order to avoid any changes on the reduced and desorbed samples. EXAFS and XANES measurements were performed at beamline X1 (HASYLAB, Hamburg). A Si(111) double crystal monochromator was used for measurements at the Pt L_{III} edge (11.564 keV). The second monochromator crystal was tilted for optimal harmonic rejection. The spectra were recorded in transmission mode with ionisation chambers filled with nitrogen and argon. The individual pressures were adjusted to optimize the signal to noise ratio. Energy calibration was performed with a platinum metal foil. To avoid mistakes in the XANES region due to small changes in the energy calibration between two measurements, all spectra were corrected to the edge position with a platinum foil, which was measured parallel to the samples between the second and third ionisation chamber.

Data evaluation started with background absorption removal from the experimental absorption spectrum by subtracting a Victoreen-type polynomial. Due to several turning points in the absorption edge, the threshold energy E₀ was determined consequently by taking the energy at half of the edge jump.^{3,4} To determine the smooth part of the spectrum, corrected for pre-edge absorption, a polynomial was used piecewise. It was adjusted in such a way that the low-R components of the resulting Fourier transform were minimal. After division of the background-subtracted spectrum by its smooth part, the photon energy was converted to photoelectron wave numbers k. The resulting $\chi(k)$ -function was weighted with k³ and Fourier transformed using a Henning window function. Data analysis was performed in k-space on unfiltered data.

Fitting was performed using the familiar theoretical EXAFS expression

$$\chi(k) = \sum_j \frac{N_j}{kr_j^2} S_0^2(k) F_j(k) e^{-2k^2\sigma_j^2} e^{-2r_j/\lambda} \sin[2kr_j + \delta_j(k)]$$

according to the curved wave formalism of the EXCURV98 program with XALPHA phase and amplitude functions.⁵ The mean free path of the scattered electrons was calculated from the imaginary part of the potential (VPI set to -4.00 eV). The

same amplitude reduction factor as achieved in a previous study was used.⁶ An inner potential correction E_f was introduced when fitting experimental data with theoretical models that account for an overall phase shift between the experimental and calculated spectra.

In the fitting procedure, care was taken that the number of fitted parameters (N_{pars}) did not exceed the degrees of freedom (N_{ind}) which are calculated according to $N_{\text{ind}} = (2\Delta k \Delta R / \pi)$.⁷ The applied ranges were $\Delta k = 15 - 4 \text{ \AA}^{-1} = 11 \text{ \AA}^{-1}$ and $\Delta R = 2.5 \text{ \AA}$. The quality of fit is given in terms of the R-factor according to⁸

$$R = \sum_i \frac{k^3 |\chi^{\text{exp}}(k_i) - \chi^{\text{theo}}(k_i)|}{k^3 |\chi^{\text{exp}}(k_i)|} \cdot 100\%$$

Experimental EXAFS data:

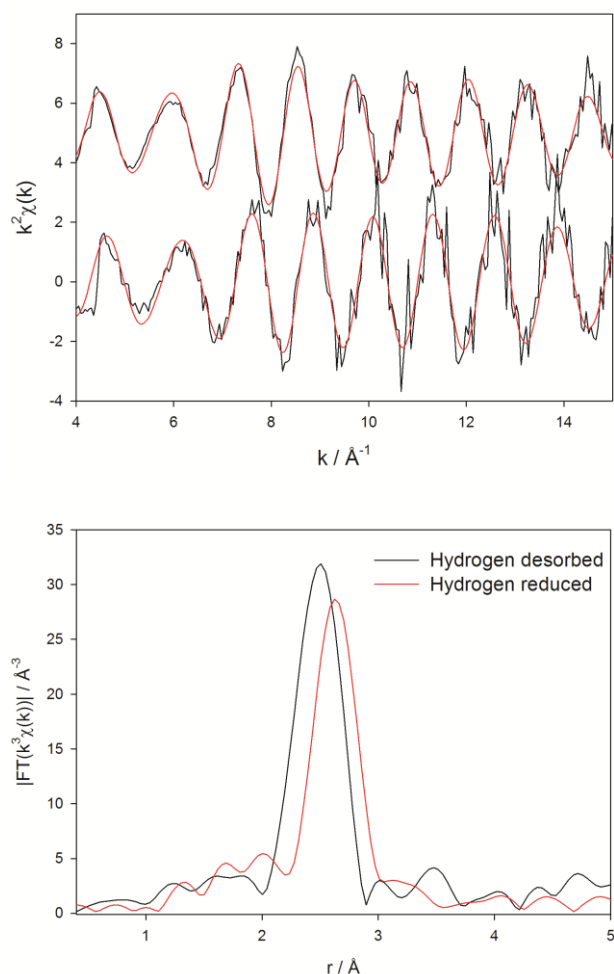


Figure S3 (Top) Experimental EXAFS functions (black) for the hydrogen desorbed sample (bottom) and hydrogen reduced sample (top) together with the corresponding fits (red). **(Bottom)** Corresponding Fourier transformed functions showing nicely the shift of the main peak.

In Figure S4, the XANES spectra of the hydrogen reduced and desorbed samples in comparison to bulk platinum are shown. According to Behafarid *et al.*,⁹ the rather large shift of the white line compared to bulk platinum is characteristic of very small clusters. Moreover, while in the hydrogen reduced sample the signature of icosahedral Pt_{13} at around 11.575 keV is clearly visible,¹⁰ it disappears for the hydrogen desorbed sample. Instead, considering the still apparent large shift compared to bulk Pt, the XANES spectrum is now characteristic of a flat cluster geometry.⁹ Again, as already pointed out in the main text, a significant fraction of larger clusters can be ruled out based on these results, since this would lead to a much smaller shift in the XANES spectra.

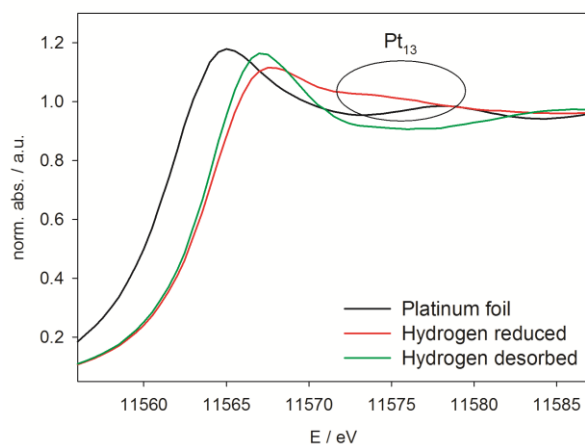


Figure S4 XANES spectra of the hydrogen reduced and desorbed samples in comparison to bulk platinum. The spectral signature of the Pt₁₃ cluster after the white line is highlighted.

References:

- 1 K. Dyrek and M. Che, *Chem. Rev.* 1997, **97**, 305.
- 2 T. Schmauke, R.-A. Eichel, A. Schweiger and E. Roduner, *Phys. Chem. Chem. Phys.*, 2003, **5**, 3076.
- 3 T. S. Ertel, H. Bertagnolli, S. Hückmann, U. Kolb, D. Peter, *Appl. Spectrosc.*, 1992, **46**, 690.
- 4 M. Newville, P. Livins, Y. Yacoby, J. J. Rehr, E. A. Stern, *Phys. Rev. B*, 1993, **47**, 14126.
- 5 S. J. Gurman, N. Binsted, I. Ross, *J. Phys. C.*, 1984, **17**, 143.
- 6 X. Liu, M. Bauer, H. Bertagnolli, E. Roduner, J. van Slageren, F. Phillipp, *Phys. Rev. Lett.*, 2006, **97**, 253401-1.
- 7 E. A. Stern, *Phys. Rev. B*, 1993, **48**, 9825.
- 8 N. Binsted, (F. Mosselman, Ed.) EXCURV98: *CCLRC Daresbury Laboratory computer program*, Manual, 1998.
- 9 F. Behafarid, L. K. Ono, S. Mostafa, J. R. Croy, G. Shafai, S. Hong, T. S. Rahman, S. R. Bare, B. R. Cuenya, *Phys. Chem. Chem. Phys.*, 2012, **14**, 11766.
- 10 F. Wen, H. Bönemann, R. J. Mynott, B. Spliethoff, C. Weidenthaler, N. Palina, S. Zinoveva, H. Modorow, *Appl. Organometal. Chem.*, 2005, **19**, 827.

